AIP Applied Physics Letters

The understanding of the drain-current fluctuation in a silicon-carbon source-drain strained n-channel metal-oxide-semiconductor field-effect transistors

E. R. Hsieh and Steve S. Chung

Citation: Applied Physics Letters **104**, 203503 (2014); doi: 10.1063/1.4879244
View online: http://dx.doi.org/10.1063/1.4879244
View Table of Contents: http://scitation.aip.org/content/aip/journal/apl/104/20?ver=pdfcov
Published by the AIP Publishing

Articles you may be interested in
Carrier transport in strained N-channel field effect transistors with channel proximate silicon-carbon source/drain stressors
Appl. Phys. Lett. **97**, 032111 (2010); 10.1063/1.3465661

The proximity of the strain induced effect to improve the electron mobility in a silicon-carbon source-drain structure of n-channel metal-oxide-semiconductor field-effect transistors
Appl. Phys. Lett. **96**, 093501 (2010); 10.1063/1.3340926

Impacts of a polycrystalline-silicon buffer layer on the performance and reliability of strained n -channel metal-oxide-semiconductor field-effect transistors with SiN capping
Appl. Phys. Lett. **90**, 122110 (2007); 10.1063/1.2715122

Secondary ion mass spectrometry characterization of source/drain junctions for strained silicon channel metal–oxide–semiconductor field-effect transistors
J. Vac. Sci. Technol. B **22**, 327 (2004); 10.1116/1.1640659

Hooge parameter in buried-channel metal-oxide-semiconductor field-effect transistors
J. Appl. Phys. **91**, 1378 (2002); 10.1063/1.1434543

This article is copyrighted as indicated in the article. Reuse of AIP content is subject to the terms at: http://scitation.aip.org/termsconditions. Downloaded to IP: 140.113.38.11 On: Thu, 25 Dec 2014 02:50:29

APPLIED PHYSICS LETTERS **104**, 203503 (2014)

The understanding of the drain-current fluctuation in a silicon-carbon source-drain strained n-channel metal-oxide-semiconductor field-effect transistors

E. R. Hsieh and Steve S. Chung[a)]
Department of Electronics Engineering and Institute of Electronics, National Chiao Tung University, Hsinchu, Taiwan

(Received 12 March 2014; accepted 5 May 2014; published online 22 May 2014)

In a certain class of strained n-channel metal-oxide-semiconductor field effect transistor (MOSFET) with silicon-carbon (Si:C) as a stressor in its source/drain, it serves as good candidate for high mobility and drain current device. However, its drain current (I_d) fluctuation and the threshold voltage (V_{th}) fluctuation, have not been clarified. This paper reports a systematic method to analyze the sources of the above two different fluctuations represented by σI_d and σV_{th}, respectively. The dominant sources of the σI_d and σV_{th} have been clarified on experimental n-channel Si:C source/drain FETs. The I_d fluctuation relies on the dopant fluctuation or the mobility factors related to the conductions at various biases. Results show that the I_d fluctuation at low field or low gate bias, i.e., near the threshold, is dominated by the RDF (Random Dopant Fluctuation) effect, while at high field, it is dominated by the channel conduction and scattering events which can be adequately described by the changes of mobility. The abnormal increase in the RDF effect in the Si:C was induced by the carbon out-diffusion from the drain into the channel. A dopant profiling technique has been developed to validate the out-diffusion effect. *© 2014 AIP Publishing LLC*. [http://dx.doi.org/10.1063/1.4879244]

For the scaling of complementary metal-oxide semiconductor field effect transistor (MOSFET) to extend the Moore's Law,[1] the enhancement of the channel mobility by various strain techniques has been the most successful one which has lasted for several generations.[2–5] Among them, the process-induced strain has gained more popularity.[6–12] In p-channel MOSFET, the usage of silicon-germanium (SiGe) in the source/drain(S/D)[6–9] has been in the production. In n-channel MOSFET, silicon-carbon (Si:C) in S/D with a tensile-strain effect becomes feasible as a counter part in the CMOS architecture.[6,10–12] On the other hand, in the further scaling of these devices, one of the major issues is the threshold voltage fluctuation caused by the random dopant fluctuation (RDF) because the electrical characteristics of the device become more sensitive to the number of dopants in the channel as we reduce the device area further.[13] Different configurations of dopant positions will affect the local threshold voltage, V_{th}, in the channel, and the electrical characteristics will not be uniform any more while the numbers of dopants are reduced to quite a few.[14]

To probe into the random dopant induced fluctuation, the most simplest way is to use the standard deviation of measurable V_{th}, such as the Pelgrom plot[15] or Takeuchi plot,[16] by the using of σVth, the standard deviation of threshold voltage, versus the device area plot as a gauge of the RDF induced effect. Also, in more recent years, more attentions have been focused on how to reduce the V_{th} fluctuation through the process or transistor architecture improvement.[17] However, the understanding of the strain effect on the drain-current (I_d) fluctuation is more important and has been rather limited. Therefore, we are really in short of a systematic approach to analyze the random dopant distribution and to understand fully the correlation between the random dopant and the fluctuations of the drain current (I_d), especially for the strain-silicon devices.

In this paper, it is of interest to understand the origin which induces the V_{th} or I_d fluctuation and to investigate the associated physical mechanisms. The V_{th} fluctuation depends on the random dopant fluctuation, while the I_d fluctuation depends on the carrier conduction or the applying field, which will both be justified experimentally. The study has been demonstrated on the strained n-channel Si:C source/drain devices.

Figures 1(a) and 1(b) are the schematics of a control and a strained Si:C source/drain n-channel MOSFET formed by the solid phase epitaxy implanted with Si:C[18] in the source/drain (S/D) region. The substitutional carbon concentrations with 1.1% in the Si:C were prepared at the condition of 950 °C and 1 ms. The dimensions of both devices are 100 nm in width, 50 nm in length, and the gate oxide is oxynitride (SION), whose equivalent oxide thickness (EOT) is 2 nm. Based on the experimental observations of the $I_d - V_{gs}$ characteristics in Fig. 1(c) for the control (conventional silicon S/D) and strained Si:C devices, these curves exhibit a horizontal shift and a vertical shift with the change of slopes. The horizontal shift is regarded as the V_{th} fluctuation (σV_{th}), while the vertical shift comes from the changes of transconductance (g_m). In the subthreshold region, the horizontal shift, σVth = 26 mV for Si:C and σVth = 18 mV for the control, reveals that the shift in σI_d of strained devices is larger than that of control ones. This is believed to the difference in the Vth fluctuation of two devices. On the contrary, in the linear region as we increase the bias, V_{gs}, σI_d of strained devices (=8%) is adversely

a)schung@cc.nctu.edu.tw

This article is copyrighted as indicated in the article. Reuse of AIP content is subject to the terms at: http://scitation.aip.org/termsconditions. Downloaded to IP: 140.113.38.11 On: Thu, 25 Dec 2014 02:50:29

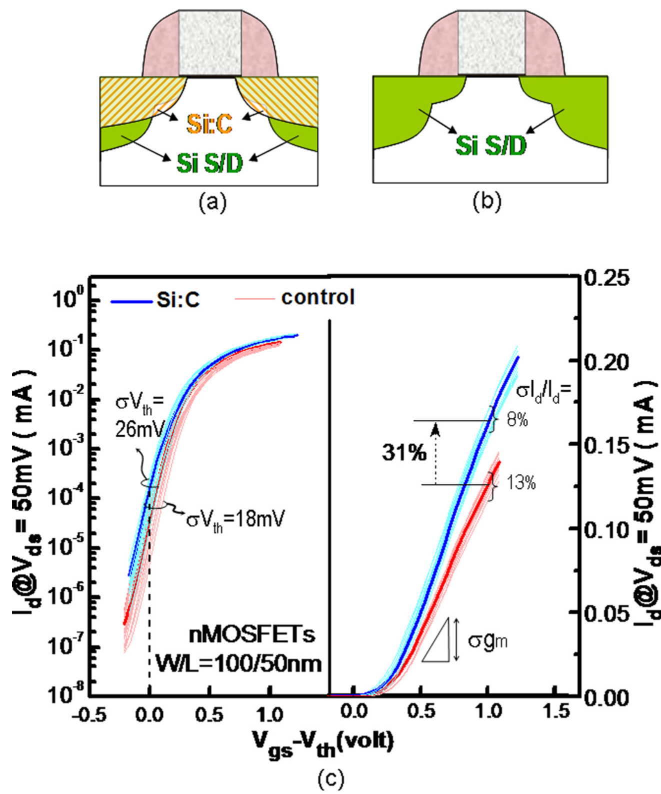

FIG. 1. The schematic of (a) a strained Si:C source/drain n-channel FET and (b) a conventional Si source/drain as a control sample, for comparison purpose. (c) The comparison of drain currents for two devices in (a) and (b). The curves on the left shows the comparison of σV_{th} measured at $V_{gs} - V_{th} = 0$ V or $V_{gs} = V_{th}$, indicating a larger fluctuation of σV_{th} for the Si:C device. Those curves on the right show the comparison at $V_{gs} - V_{th} = 1$ V and Si:C device exhibits a reduced I_d current fluctuation.

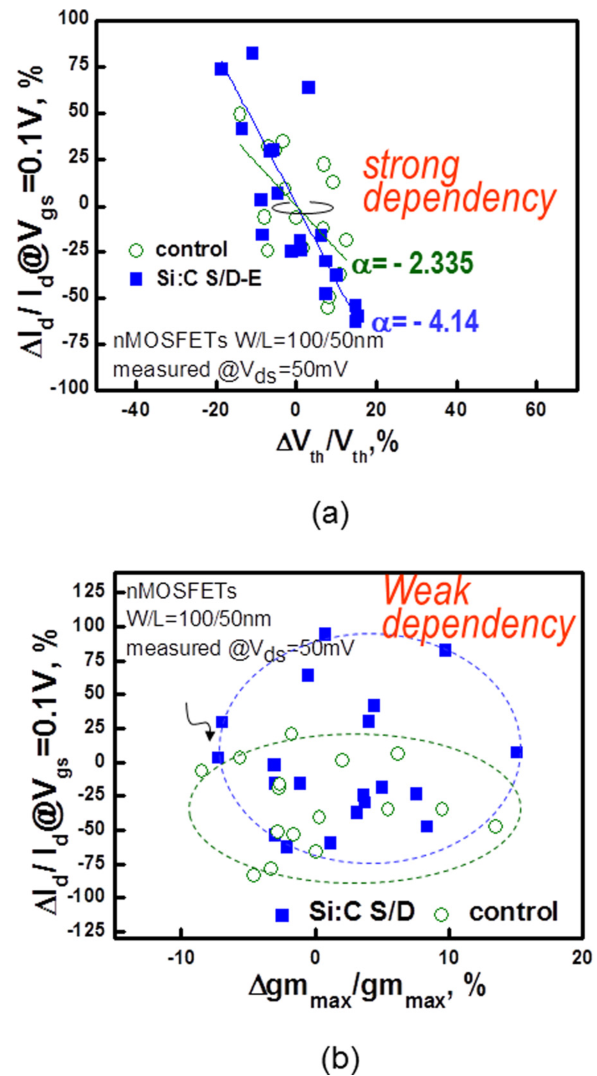

FIG. 2. The scattering plots to show the dependency of (a) the normalized drain current on the threshold voltages (normalized), (b) the normalized drain current on the maximum transconductance (normalized), at low field with $V_{gs} = 0.1$ V.

smaller than that of control devices (=13%), which cannot be adequately described by the σV_{th} apparently. To understand their discrepancies, the current I_d in the linear region can be represented by

$$I_d = (W/L)\mu_{eff} C_{ox}(V_{gs} - V_{th})V_{ds}, \quad (1a)$$

$$= g_m(V_{gs} - V_{th}), \quad (1b)$$

where W and L are the width and length of devices, respectively, μ_{eff} is the effective mobility, C_{ox} is the gate-oxide capacitance, and g_m is defined as the derivative of I_{ds} to V_{gs}, e.g., $g_m = \partial I_{ds}/\partial V_{gs} = (W/L)\ \mu_{eff}\ C_{ox}V_{ds}$. Therefore, I_d can be expressed in terms of g_m and V_{th} as shown in Eq. (1b). Both factors are responsible for the horizontal and the vertical shift of the I_d shown in Fig. 1(c). Furthermore, the standard deviation of normalized $I_d(\sigma\overline{I_d})$ can be further represented by

$$\sigma\overline{I_d} = \sqrt{\left(\alpha \times \sigma\overline{V_{th}}\right)^2 + \left(\beta \times \sigma\overline{g_m}\right)^2}, \quad (2)$$

in which α is the dependent factor of $\sigma\overline{I_d}$ and β is the dependent factor of $\sigma\overline{g_m}$. Figs. 2(a) and 2(b) are the scattering plots of normalized I_d versus V_{th} and gm_{max}, respectively, in the subthreshold regime at $V_{gs} = 0.1$ V, whose slopes represent α and β. In comparison, the plots show a stronger dependency on α in comparison to the β, i.e., the dominant fluctuation source of I_d in the subthreshold region is V_{th}, corresponding to the parallel shift in Fig. 1(c). Moreover, it is noted that σV_{th} of strained devices ($|\alpha| = 4.14$) is larger than that of control one ($|\alpha| = 2.335$), as given in Fig. 2(a). This is believed to be the specific Si:C structure which induces larger σV_{th}.

In order to understand why Si:C S/D devices raised a larger σV_{th}, which results in a severe σI_d in the subthreshold region, Fig. 3(a) shows Pelgrom plot, where the standard deviation of V_{th} against the inverse of square-root of device area, and its slope, A_{vt}, can be considered as the degree of σV_{th}. In other words, larger slope exhibits much larger RDF. It shows that σV_{th} is getting worse when the strain is introduced in the drain/source with carbon. In lieu of the methodology that authors demonstrated,[19] a so-called discrete dopant profiling technique (DDP) can be used to examine why Si:C device has higher RDF induced V_{th} fluctuation. The main idea of DDP is described as below. If the discrete dopant is treated as a delta function located in the channel randomly, only those discrete dopants at the channel barrier peak will contribute to the V_{th} variation, i.e.,

This article is copyrighted as indicated in the article. Reuse of AIP content is subject to the terms at: http://scitation.aip.org/termsconditions. Downloaded to IP: 140.113.38.11 On: Thu, 25 Dec 2014 02:50:29

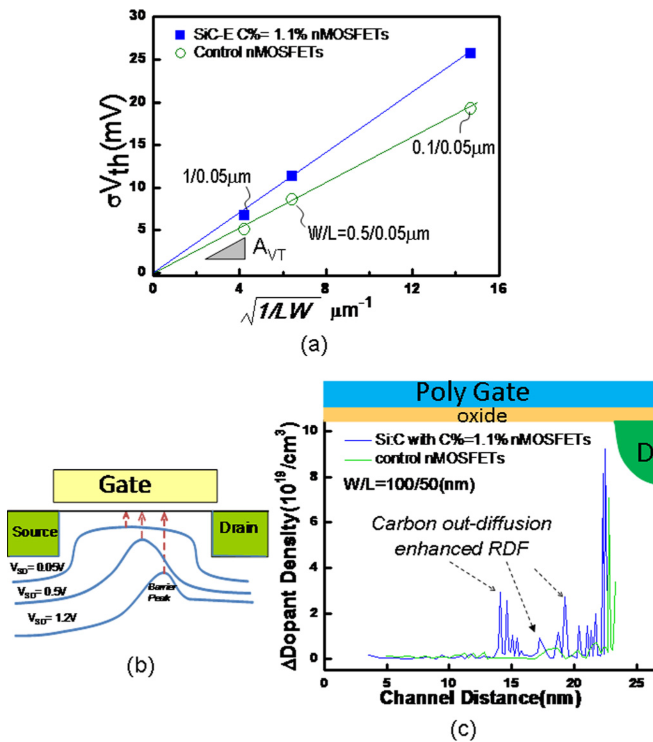

FIG. 3. (a) The Pelgrom plot of the tested samples with different channel widths but a fixed channel length. Note that the slope A_{VT} is a measure of the σV_{th}. (b) The schematic to describe the profiling of channel dopant densities. (c) The experimental results of dopant distributions for both the Si:C S/D device (blue color) and the control (green color). The high peaks in the channel are the carbon out-diffusion enhanced RDF.

$$\sigma V_{th} = (q/C_{ox})\sqrt{\left(\int_0^{W_d} \Delta n_i(x)\delta(x - x_i)dx\right)\Big/LW}, \quad (3)$$

$$= (q/C_{ox})\sqrt{\sum \Delta n_i(x)/LW}. \quad (4)$$

Here, q is a constant value, 1.6×10^{-19} with unit of coulomb, $\Delta n_i(x)$ is the varying amount of dopant density, n_i, and $\delta((x - x_i))$ is Dirac delta function, with unity of its integral at x_i but zero elsewhere. Since the σV_{th} is directly related to the summation of each discretized varying amount, $\Delta n_i(x_i)$, the variation of dopant density at a specified location, i.e., $\Delta N_i(x)$, can be derived as

$$\Delta N_i(x) = (C_{ox}\sigma V_{th}/q)^2 \quad (\text{unit: number/cm}^3). \quad (5)$$

Experimentally, by increasing the source-to-drain voltage, V_{sd}, the channel barrier peak will be moved from the middle of the channel to the region near the drain side in Fig. 3(b), from which the location of dopant density can be determined along the channel direction by calculating the barrier peak position. In other words, from the calculation of channel barrier peak position, we can calculate the variation of dopant density as a function of the channel position from the measured σV_{th}. Fig. 3(c) shows the results of the dopant densities along the channel. There are high peaks of the dopant densities in the channel in the Si:C device. This is believed to be the carbons out-diffused into the channel from the Si:C S/D region, which induces the RDF effect. In other words, these carbons in the channel do not occupy the substitutional sites but are considered to be the defects in the channel and cause the perturbation of the channel potential, resulting in a larger boron atom fluctuation or V_{th} variation. This is consistent what we measured in the Pelgrom plot, Fig. 3(a), that Si:C device shows a larger A_{VT} value. Meanwhile, in Fig. 3(c), we also found that huge peaks close to the drain edge were observed. It is due to the fact that not only the carbons but also the impurities in the drain, e.g., arsenic (As), are diffused into the channel. Because the relative heavy atomic mass of arsenic, the distance of arsenic out-diffusion is very short and just around the corner of the drain edge. These high peaks are an indication of the arsenic induced fluctuation.

Furthermore, when we increase the gate bias above V_{th}, the vertical drain-current variation becomes more fluctuated than the horizontal one, as can be clearly seen from the right hand side curves in Fig. 1(c) where Si:C device exhibits a small σI_d, which is no longer dominated by V_{th}, and rather there would have another factor which creates the differences. Figures 4(a) and 4(b) are the scattering plots of normalized V_{th} and gm_{max} versus I_d at $V_{gs} = 1$ V, respectively. In

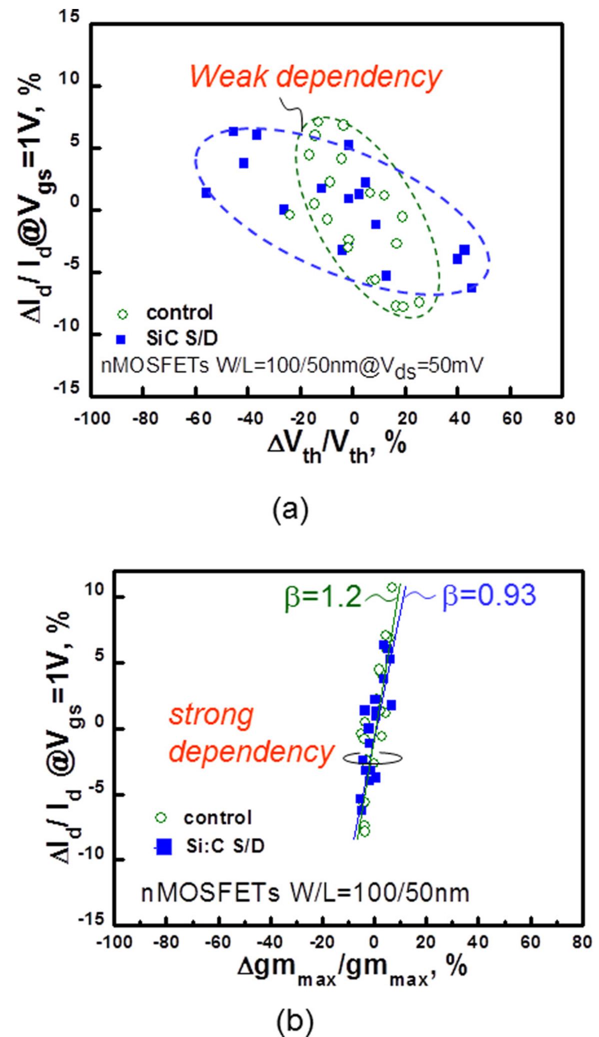

FIG. 4. The scattering plots to show the dependency of (a) the normalized drain current on the threshold voltages (normalized), (b) the normalized drain current on the maximum transconductance (normalized), at high field with $V_{gs} = 1$ V.

This article is copyrighted as indicated in the article. Reuse of AIP content is subject to the terms at: http://scitation.aip.org/termsconditions. Downloaded to IP: 140.113.38.11 On: Thu, 25 Dec 2014 02:50:29

contrast to Fig. 2, it was found that gm_{max} exhibits stronger dependency on I_d, but V_{th} shows weaker dependency. Thus, *gm_{max} is more significant than V_{th} in terms of their contributions to σI_d at higher field*. To justify the above observations, Fig. 5(a) shows the comparisons of normalized standard deviations of gm_{max} for two devices. It was found that the Si:C exhibits a smaller σgm_{max} value such that its σI_d is smaller. This is consistent with the comparison in Fig. 4(b). Moreover, the curves of σgm in Fig. 5(a) show a three-segment trend, which corresponds to a three-segment trend of mobility characteristics as V_{gs} is varied in Fig. 5(b). Therefore, the fluctuation source of gm can be considered to be mainly from the scattering of mobility. When the channel is in weak-inversion at low V_{gs}, impurity scattering is dominant, which determines the carrier scattering and exhibits a very higher σgm. While at V_{gs} just slightly higher than V_{th}, the channel impurity is shielded by the inversion-charge, the phonon scattering takes place and dominates σgm. Because the mobility is the highest in this region, σgm is the lowest with relatively low scattering events. When V_{gs} is raised much higher than V_{th}, mobility decreases while surface roughness scattering increases and σgm is increased simultaneously. In other words, the fluctuation source of gm is believed to be from phonon scattering or surface scattering of the mobility at high filed, i.e., $V_{gs} > V_{th}$.

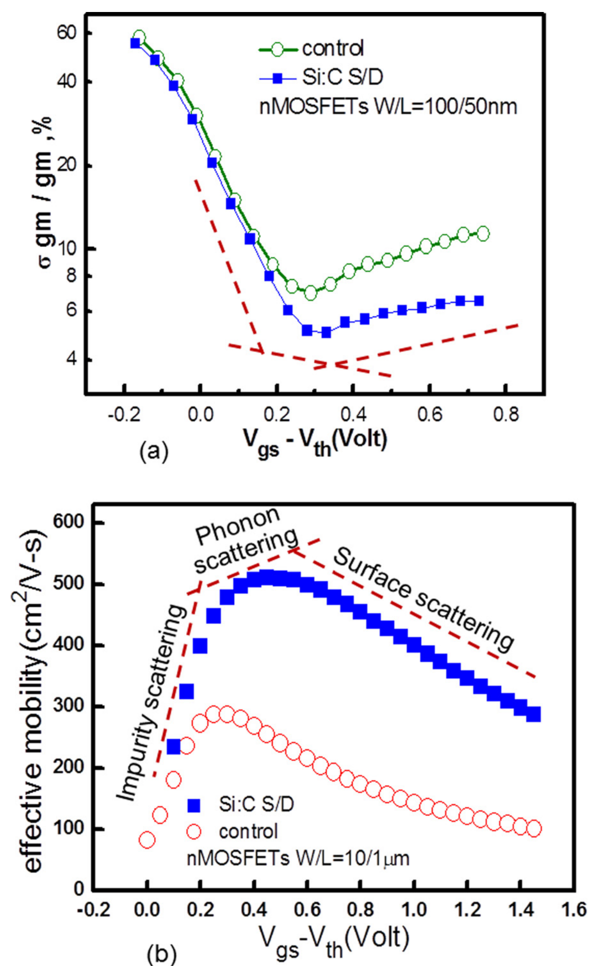

FIG. 5. (a) The dependence of the transconductance variation, σgm/gm, on the applied gate biases from low field to high field. (b) The comparison of mobilities between the strained Si:C device and the control device in which the dependencies on the gate biases exhibit a three-segment trend corresponding to three different physical mechanisms.

In short, the addition of carbon in the Si:C introduced the strain and provides a current gain of 41% (Fig. 1(c)) and a better σId in the device operating voltage ranges of interest, nevertheless the penalty is a higher V_{th} variation in the subthreshold region of I_d. Extra efforts may be taken to have a good control of the incorporation of carbon in the source/drain through the process improvement.

In conclusion, an experimental methodology has been provided to analyze the fluctuation sources of I_d systemically. It was demonstrated on a specific class of strained devices with Si:C source/drain structure. The I_d fluctuation can be decoupled into g_m and V_{th} fluctuations depending on the device operating regions. The V_{th} dominates σI_d at low field (subthreshold region), while g_m dominates at high field (linear region). By introducing the carbon in the Si:C structure, it has been able to suppress the carrier scattering and reduce the g_m fluctuation dramatically, leading to a much lower I_d fluctuation in comparison to the control devices at high field. *This is good for a device by using the strain in the enhancement of mobility*. However, it has adversely induced larger Vth fluctuation at low field, i.e., V_{th} served as the dominant fluctuation source of I_d in the subthreshold region. This was attributed to the carbon-out-diffusion enhanced dopant fluctuation in the channel, which can be reasonably justified by the proposed dopant profiling technique. Although the methodology was demonstrated specifically on the strained devices, it can also be very useful and to be applied to any miniaturized MOSFETs to examine their I_d and V_{th} fluctuations.

This work was support in part by the National Science Council, Taiwan, under Contract *NSC100-2221-E009-016-MY3* and NCTU-UCB I-RiCE program, Ministry of Science and Technology, Taiwan, under Grant No. MOST 103-2911-I-009-302.

[1]G. Moore, Electronics **38**, 114 (1965).
[2]S. E. Thompson, G. Sun, Y. S. Choi, and T. Nishida, IEEE Trans. Electron Devices **53**, 1010 (2006).
[3]S. E. Thompson and S. Parthasarathy, Mater. Today **9**, 20 (2006).
[4]Y. Sun, S. E. Thompson, and T. Nishida, J. Appl. Phys. **101**, 104503 (2007).
[5]B. Yang and M. Cai, Sci. China Inf. Sci. **54**, 946 (2011).
[6]K.-W. Ang, K.-J. Chui, V. Bliznetsov, C.-H. Tung, A. Du, N. Balasubramaniam, G. Samudra, M. F. Li, and Y.-C. Yeo, Appl. Phys. Lett. **86**, 093102 (2005).
[7]P. R. Chidambaram, C. Bowen, S. Chakravathi, C. Machala, and R. Wise, IEEE Trans. Electron Devices **53**, 944 (2006).
[8]K. Mistry, M. Armstrong, C. Auth, S. Cea, T. Coan, T. Ghani, T. Hoffmann, A. Murthy, J. Sandford, R. Shaheed, K. Zawadzki, K. Zhang, S. Thompson, and M. Bohr, Symp. VLSI Technol., Dig. Tech. Pap. **2004**, 50.
[9]S. S. Chung, D. C. Huang, Y. J. Tsai, C. S. Lai, C. H. Tsai, P. W. Liu, Y. H. Lin, C. T. Tsai, G. H. Ma, S. C. Chien, and S. W. Sun, Int. Electron Devices Meet. **2006**, 325.
[10]S. S. Chung, E. R. Hsieh, D. C. Huang, C. S. Lai, C. H. Tsai, P. W. Liu, Y. H. Lin, C. T. Tsai, G. H. Ma, S. C. Chien, and S. W. Sun, Int. Electron Devices Meet. **2008**, 435.
[11]K.-W. Ang, K.-J. Chui, V. Bliznetsov, A. Du, N. Balasubramaniam, G. Samudra, M. F. Li, and Y.-C. Yeo, Int. Electron Devices Meet. **2004**, 1069.
[12]B. Yang, R. Takalkar, Z. Ren, L. Black, A. Dube, J. W. Weijtmans, J. Li, J. B. Johnson, J. Faltermeier, A. Madan, Z. Zhu, A. Turansky, G. Xia, A. Chakravarti, R. Pal, K. Chan, A. Reznicek, T. N. Adam, B. Yang, J. P. de Souza, E. C. T. Harley, B. Greene, A. Gehring, M. Cai, D. Aime, S. Sun, H. Meer, J. Holt, D. Theodore, S. Zollner, P. Grudowski, D. Sadana,

This article is copyrighted as indicated in the article. Reuse of AIP content is subject to the terms at: http://scitation.aip.org/termsconditions. Downloaded to IP: 140.113.38.11 On: Thu, 25 Dec 2014 02:50:29

D.-G. Park, D. Mocuta, D. Schepis, E. Maciejewski, S. Luning, J. Pellerin, and E. Leobandung, Int. Electron Devices Meet. **2008**, 1–4.
[13]T. Mizuno, J. Okamura, and A. Toriumi, IEEE Trans. Electron Devices **41**, 2216 (1994).
[14]I. D. Mayergoyz and P. Andrei, J. Appl. Phys. **90**, 3019 (2001).
[15]M. J. M. Pelgrom, A. C. J. Duinmaijer, and A. P. G. Welbers, IEEE J. Solid-State Circuits **24**, 1433 (1989).
[16]K. Takeuchi, T. Fukai, T. Tsunomura, A. T. Putra, A. Nishida, S. Kamohara, and T. Hiramoto, Int. Electron Devices Meet. **2007**, 467.
[17]K. Kuhn, Sci. China, Inf. Sci. **54**, 936 (2011).
[18]E. R. Hsieh and S. S. Chung, Appl. Phys. Lett. **96**, 093501 (2010).
[19]E. R. Hsieh, S. S. Chung, C. H. Tsai, R. M. Huang, C. T. Tsai, and C. W. Liang, Symp. VLSI Technol., Dig. Tech. Pap. **2011**, 184.

This article is copyrighted as indicated in the article. Reuse of AIP content is subject to the terms at: http://scitation.aip.org/termsconditions. Downloaded to IP: 140.113.38.11 On: Thu, 25 Dec 2014 02:50:29